

Metformin Decreases the Expression of VEGF-A and CTGF-1 and Improves Histological, Ultrastructural and Hormonal Changes in Adult Rat Polycystic Ovary

Ghalia Mahfouz ATTIA, Rasha Ahmed ELMANSY, and Mohamed H. ELSAYED

Accepted February 28, 2019

Published online March 26, 2019

Issue online March 29, 2019

Original article

ATTIA G.M., ELMANSY R.A., ELSAYED M.H. 2019. Metformin decreases the expression of VEGF-A and CTGF-1 and improves histological, ultrastructural and hormonal changes in adult rat polycystic ovary. *Folia Biologica (Kraków)* 67: 25-43.

In this study we explored the possible beneficial role of metformin (MT) treatment on the hormonal, histological and ultrastructural changes in testosterone propionate induced polycystic ovary (PCO) in rats. A total of 45 female adult rats were divided into control, PCO and MT-PCO groups. After 28 days of treatment, blood samples were taken for estimation of glucose, insulin, sex hormones as well as insulin resistance (IR) and insulin sensitivity (IS) indices (HOMA-IR & QUICKI-IS). Ovarian tissues were processed for light and electron microscopic studies. Also, immunohistochemical stains were done for detection of vascular endothelial growth factor-A (VEGF-A) and connective tissue growth factor-1 (CTGF-1). The PCO group showed a decrease in follicle number with a predominance of cystic follicles, absence of corpora lutea, decrease in the thickness of granulosa cells and increased thickness of theca interna cells layers, hypercellularity of interstitial stroma, as well as increased expression of VEGF-A and CTGF-1. Ultrastructurally, signs of granulosa cell degeneration and luteinization of theca interna cells were noted. Additionally, an increase in the serum concentration of estrogen, testosterone, insulin, IR and a decrease in progesterone and IS were also observed. MT treated PCO group showed improvement of the above-mentioned changes. These data provide new insight about the promising effect of MT in treatment for PCOS associated infertility.

Key words: Polycystic ovary, metformin, VEGF, CTGF, ultrastructure, insulin sensitivity.

Ghalia Mahfouz ATTIA[✉], Department of Anatomy, Faculty of Medicine, Taibah University, Al Madina Al Monawarra, KSA; Department of Histology and Cell Biology, Faculty of Medicine, Mansoura University, Egypt.

E-mail: drghalia2011@gmail.com

Rasha Ahmed ELMANSY, Department of Anatomy and Embryology, Faculty of Medicine, Ain Shams University, Cairo, Egypt; Department of Anatomy, Faculty of Medicine, Unaizah College of Medicine, AlQassim University KSA.

Mohamed H. ELSAYED, Department of Physiology, Faculty of Medicine, Ain Shams University, Cairo, Egypt.

Polycystic ovary syndrome (PCOS) is a widespread multifactorial endocrinological disease up-setting 6-10% of women in the reproductive age (NORMAN *et al.* 2007) and it is supposed to be one of the globally most important causes of anovulatory infertility (BARTHELMESS & NAZ 2014). PCOS refers to a disorder with a mixture of unique reproductive and metabolic features such as hyperandrogenism, enlarged polycystic ovaries on ultrasound scan, disturbance of ovulatory function, hirsutism and acne (CARMINA *et al.* 2010). In addition, symptoms of metabolic syndrome such

as obesity, insulin resistance and hyperinsulinemia are frequently seen in a greater number of women with PCOS (GAMBINERI *et al.* 2002; OLLILA *et al.* 2017).

However, the precise pathophysiology of this endocrinopathy has not been elucidated. IR is thought to be one of its major causes, particularly in obese individuals. IR causes an increase in the level of serum insulin, which interacts with the luteinizing hormone (LH) contained by the ovarian theca cells, resulting in a considerable rise in the cholesterol level, a decline in glucose transport, an

augmented formation and discharge of androgens, and finally childlessness (BARBER *et al.* 2015). This disorder is also associated with an increased possibility of type 2 diabetes mellitus, dyslipidemia, heart diseases, emotional distress, preeclampsia, endometrial hyperplasia and endometrial cancer (VELTMAN-VERHULST *et al.* 2012; DUMESIC & LOBO 2013; GOODMAN *et al.* 2015).

Accordingly, IR in PCOS has led to the application of a key novel curative approach based on insulin sensitizers such as metformin (MT) which has multiple established and developing applications in women's reproductive health. MT is a stable biguanide low molecular weight oral anti-hyperglycemic drug. It decreases blood glucose, intestinal glucose absorption and suppresses hepatic gluconeogenesis (SIVALINGAM *et al.* 2014). Besides, the drug also lowered insulin levels, LH production, circulating androgen levels, improved ovulation, pregnancy probabilities and fertility outcomes in clomiphene citrate resistant PCO women (TANG *et al.* 2012).

Moreover, increased insulin sensitivity by MT improved health-related quality of life of PCOS women by relieving emotional troubles (OU *et al.* 2016). Also, administration of MT for 3 months prior to *in vitro* fertilization or intracytoplasmic sperm injection improved live birth rates (KJØTRØD *et al.* 2011). Furthermore, MT lowered the chance of commencement of gestational diabetes mellitus in PCOS women and seemed to be a superior tool in metabolic control compared to insulin and other oral antidiabetic agents during pregnancy (ROJAS *et al.* 2014).

Connective tissue growth factor (CTGF) has been gradually considered as a new indicator for detection of tissue fibrosis. CTGF belongs to the CCN family, which comprise many polypeptide factors with high homology in their DNA sequences. This factor is a cysteine-rich cytokine formed in the ovary by follicular granulosa cells and fibroblasts which showed similar biological functions to TGF- β 1 (ZHOU *et al.* 2017). Expression of CTGF messenger RNA was discovered in preantral follicles and early antral follicles in rat ovaries. Granulosa cell-derived CTGF plays a significant role in theca cell employment, follicle growth and corpus luteum vascularisation. Also granulosa cell CTGF gene expression is inversely linked to the phase of granulosa cell differentiation (HARLOW *et al.* 2002). ZHANG *et al.* (2013) detected increased expression of CTGF in the ovarian and uterine tissues of PCO rats. It promotes cell proliferation, collagen synthesis, expression of cell adhesion molecules, and extra cellular matrix (ECM) production in different cells. Each of these important functions create awareness to the vital role of CTGF in numerous diseases associated

with tissue reconstitution, for example in wound healing, fibrosis, and tumorigenesis (ALFARO *et al.* 2013; LAI *et al.* 2013; ROMÃO *et al.* 2013). However, the precise role of CTGF in ovarian tissues is still unclear.

Vascular endothelial growth factor (VEGF) is a multifunctional cytokine that is expressed in both ovary and endometrium. As soon as it combines with its receptor, an increase in the number and growth of vascular endothelial cells occurs. LUO *et al.* (2017) found that VEGF directly regulates several profibrotic and immune cytokine genes in hepatic stellate cells. It has also been reported that the ovarian volume and antral follicle count are positively correlated with the concentration of VEGF (ZHAO *et al.* 2010). So, supplementary research is needed to detect their specific mechanisms and possible role in ovarian tissue. Therefore, the aim of the present study was to explore the possible beneficial role of the insulin sensitizer MT on the hormonal, histological and ultrastructural changes in induced PCO in adult rats and to elucidate its impacts on the expression of CTGF and VEGF in this syndrome.

Materials and Methods

Abbreviations:

- MT – metformin.
- IR – insulin resistance.
- IS – insulin sensitivity.
- HOMA-IR – homeostasis model assessment of insulin resistance.
- QUICKI – quantitative insulin sensitivity check index.
- TP – testosterone propionate.
- BMI – body mass index.
- BWG – body weight gain.

Animals

Forty five adult (12 weeks of age) female albino rats weighing 180-200 g were used for the study. Animals were purchased from the animal house of the Medical Research Center, Faculty of Medicine, Ain Shams University. Rats were kept in a well-ventilated room one week before initiating the experiment for acclimatization at room temperature of 28°C and 12:12 light/dark cycle. They were fed standard rat chow and tap water *ad libitum*. The experiments were performed in accordance with the National Institutes of Health (NIH) guidelines for the Care and Use of Laboratory Animals. The study was approved by the local institutional experimental research committee.

Drugs

1. Testosterone propionate (TP): (Viromone 100 mg/2 ml, Recipharm Limited CO, UK).
2. Metformin (MT) (Sigma Chemical Co; USA).

Study design

The rats were equally allocated into three groups designated as:

A. PCO group (15 rats): animals were injected intraperitoneally (ip) with TP at a dose of 1 mg/100 g BW dissolved in sesame oil once daily for 28 days.

B. Control group (15 rats): animals were injected intraperitoneally (ip) with sesame oil and given distilled water orally (0.05 ml) daily for 28 consecutive days.

C. MT+PCO group (15 rats): animals were injected with 1 mg/100 g BW TP and given MT orally (50 mg/100 g BW in 0.05 ml of distilled water given orally by gavage) daily for 28 days. The dose of MT administered was equivalent to that used in the treatment of women with PCOS (WALTERS *et al* 2012; POORNIMA *et al.* 2015).

Vaginal smears

From the first day of experiment, vaginal smears were performed daily for each group to observe their estrous cycles using a cotton-tipped sterile swab. The swab was rotated two or three times against the vaginal wall and then withdrawn and rolled on a clean glass slide, stained with H&E. Smears were examined under the light microscope for detection of cornified cells, nucleated epithelial cells and leukocytes. Cycles with duration of 4-5 days were considered regular. Identification of cornified cells in the smears during a minimum of 10 serial days was defined as persistent vaginal cornification (PVC) that was considered as an indication of follicular cystic development (MARCONDES *et al.* 2002; SALVETTI *et al.* 2004)

Blood and tissue collection

After the experimental period, all rats were fasted overnight and anaesthetized with i.p. injection of sodium thiopental (40 mg/kg of body weight) (Sigma Chemical Co., ST Louis, MO, USA) (TOBLLI *et al.* 2012). Blood was collected via cardiac puncture, and fasting blood glucose for all groups was immediately estimated in part from collected blood samples, the remaining part of blood samples were then put in heparinized tubes and centrifuged (3000×g for 10 min at 4°C) to obtain sera which were kept at -20°C. Due to technical problems during collection and centrifugation of blood samples of rats of all groups, only the sera

of 30 rats (10 rats from each group) were used for blood analyses. The collected sera were later used for estimation of progesterone, estrogen, testosterone and insulin using ELISA kits (Beinglay Biotechnology Co., Ltd., Wuhan, China). The 45 rats were then sacrificed, two ovaries were excised, cleaned of fat and processed for both light and electron microscopic examination.

Study of insulin resistance and insulin sensitivity

The homeostasis model assessment-estimated insulin resistance (HOMA-IR) has been used for the estimation of insulin resistance in this experiment (MATTHEWS *et al.* 1985). It is calculated by multiplying fasting plasma insulin (FPI) by fasting plasma glucose (FPG), then dividing by the constant 22.5, i.e. $HOMA-IR = (FPI \times FPG) / 22.5$ (WALLACE *et al.* 2004). The quantitative insulin sensitivity check index (QUICKI) was used to assess the insulin sensitivity. QUICKI is derived using the inverse of the sum of the logarithms of the fasting insulin and fasting glucose: $1 / (\log(\text{fasting insulin } \mu\text{U/ml}) + \log(\text{fasting glucose mg/dl}))$ (KATZ *et al.* 2000).

Light microscopic examination

Specimens were fixed in 10% neutral buffered formalin then washed with water, dehydrated in ascending grades of ethyl alcohol, cleared in xylene, and embedded in paraffin to prepare paraffin blocks. Tissue sections (5 µm) were cut and then were mounted on glass slides, deparaffinized in xylene and stained by hematoxylin and eosin (H&E) (BANCROFT & GAMBLE 2008) for general histological examination and immunohistochemical stains for localization of VEGF-A and CTGF-1 using avidin-biotin-peroxidase complex (ABC) techniques (HSU *et al.* 1981).

Immunohistochemistry

Using the streptavidin-biotin technique, paraffin sections were deparaffinized in xylene, rehydrated, rinsed in tap water, and embedded in 3% hydrogen peroxide (H₂O₂) in phosphate buffer solution (PBS) for 10 min to block endogenous peroxidase. A monoclonal mouse anti-human antibody was used for detection of VEGF-A (Clone. SP28, Catalog No. M3281, Spring Bioscience, ready to use) and rabbit polyclonal CTGF-1 antibody (5 µg/ml; cat. no. ab125943; Abcam, Cambridge, MA, USA) was used for detection of CTGF-1. For both VEGF-A and CTGF-1 an antigen retrieval procedure was applied by pretreatment of sections for 10 min in a microwave oven in 0.01 M sodium citrate buffer (pH 6.0 followed by cooling for further 20 min). The sections were then

incubated with the corresponding primary antibodies followed by their incubation in goat anti-rabbit biotinylated secondary antibody (Vector Laboratories, Burlingame, CA) to detect them. Visualization of the tissues was obtained by using horseradish peroxidase-avidin-biotin complex (Vectastain Elite, Vector, CA) then 3,3'-diaminobenzidine in H_2O_2 (DAB kit, Vector, CA). The sections were then counterstained with haematoxylin and mounted.

Transmission EM preparation

Ovarian specimens were immediately fixed in 2.5% phosphate-buffered glutaraldehyde solution at 4°C for 24 hours, then washed over night several times with fresh solution of 0.1 M sodium phosphate buffer, PH 7.4 at 4°C. Afterwards, specimens were post-fixed in 2% osmium tetroxide in 0.1 M sodium phosphate buffer in the dark at +40°C. Specimens were dehydrated in ascending grades of ethanol and propylene oxide then embedded in resin. Semi-thin sections were made and stained with toluidine blue and examined by light microscope. Ultra-thin sections were cut at thickness of 90 nm, mounted on copper grids and stained with uranyl acetate 5% for 15 min followed by lead citrate for 8 min and examined by transmission electron microscope SEO (Sumy Electron Optics) model PEM-100 at different magnifications (GLAURET & LEWIS 1998). Transmission electron examination and photography were done at the Military Medical Academy Electron Microscope Department, Cairo, Egypt.

Morphometric study

Numbers of primordial, primary, preantral, antral, cystic follicles and corpora lutea were measured from H&E stained sections ($\times 100$). Thickness of granulosa and theca interna cell layer of preantral, antral and cystic follicles were measured from H&E stained section ($\times 400$). Area % of VEGF-A and CTGF-1 immunoexpression were measured from anti-VEGF-A and anti-CTGF-1 immunostained sections, respectively. For each of the above measured parameters, two non-overlapping fields/rat paraffin block sections were examined (the total number was 30 measurements for each group). All measured items were photographed using color video camera (digital camera CH-9435 DFC 290). In photographs of immunostained sections, the brown color of the immunoreaction in the analyzed photos was masked by a blue color using Leica Qwin 500 (Imaging System, Cambridge, UK) within a frame area of $293.4288 \mu\text{m}^2$. Area of blue color was divided on the frame area of the field to obtain the area % of the immunoreaction. Morphometry was carried out at the Image

Analysis Unit, Anatomy Department, Faculty of Medicine, Taibah University, Al Madinah Al Monawwarah, KSA.

Statistical analysis

Statistical analysis was performed using IBM SPSS software version 21.00 (Chicago, Illinois, USA). Data revealed a normal distribution (Shapiro-Wilk test) and one-way analysis of variance (ANOVA) followed by the least significant difference test (LSD) was carried out. Results are presented as mean \pm standard error of mean (SEM). Differences between groups at $p > 0.05$, $p \leq 0.05$ and $p \leq 0.001$ were considered non-significant, significant and highly significant, respectively.

Results

Biochemical results

Measurements of hormones and glucose in blood serum are presented in Table 1. A highly significant increase in the mean concentrations of serum estrogen, testosterone and fasting insulin hormones, and a highly significant decrease in progesterone concentrations were detected between PCO rats and control ($p = 0.000$). An insignificant difference between these two groups was detected in the mean concentration of fasting blood glucose ($p = 0.030$).

Additionally, insulin resistance index (HOMA-IR) was significantly elevated (3.42 ± 0.88 vs 1.40 ± 0.39) and insulin sensitivity index (QUICKI-IS) was significantly reduced (0.53 ± 0.09 vs 0.67 ± 0.08) when PCO rats were compared to control group (Table 1).

On the other hand, a highly significant decrease in the mean concentration of estrogen, testosterone and fasting insulin hormones, and highly significant increase in progesterone concentration were detected in MT-PCO rats when compared to PCO group ($p \leq 0.000$ in all cases). A significant decrease in the mean concentration of fasting blood glucose was detected ($p = 0.001$), also, HOMA-IR was highly significantly decreased ($p = 0.000$) while QUICKI-IS was significantly increased ($p = 0.01$) when MT-PCO rats were compared to PCO rats (Table 1).

Insignificant differences were observed between MT-PCO group and control group regarding serum concentrations of estrogen, progesterone, testosterone, fasting insulin hormones and fasting blood glucose, as well as values of HOMA-IR and QUICKI-IS (see Table 1).

Table 1

Mean serum concentrations of estrogen (pg/ml), progesterone (ng/ml), testosterone (ng/dl) & fasting insulin (ng/ml) hormones and fasting blood glucose (mg/dl) level and values of HOMA-IR, QUICKI-IS and body weight gain (BWG, g). Values are represented as mean \pm standard error of mean (SEM). N=10 rats for all above parameters except BWG, N=15

Group	Estrogen	Progesterone	Testosterone	Fasting insulin	Fasting blood glucose	HOMA-IR	QUICKI-IS	BWG
Control	50.60 \pm 1.52	6.56 \pm 0.18	39 \pm 0.87	0.38 \pm 0.04	83.2 \pm 1.91	1.40 \pm 0.39	0.67 \pm 0.08	29.80 \pm 0.29
PCO p1	84.60 \pm 1.94 0.000	3.98 \pm 0.24 0.000	57.70 \pm 2.06 0.000	0.86 \pm 0.10 0.000	89.40 \pm 2.41 0.030	3.42 \pm 0.88 0.000	0.53 \pm 0.09 0.01	42.48 \pm 0.86 0.000
MT-PCO p2 p3	56.30 \pm 1.43 0.000 0.021	5.73 \pm 0.32 0.000 0.032	40.40 \pm 0.920 0.000 0.484	0.44 \pm 0.05 0.000 0.557	79.70 \pm 1.23 0.000 0.207	1.56 \pm 0.62 0.000 0.483	0.65 \pm 0.11 0.000 0.92	25.77 \pm 0.47 0.000 0.000

p: Probability

p1: significance between control and PCO groups.

p2: significance between PCO and MT-PCO groups.

p3: significance between control and MT-PCO groups.

Despite the insignificant differences among all studied groups regarding their initial body weight (BW), BW gain (BWG) at the day of sacrifice was significantly higher in the PCO group compared to the control group ($p = 0.000$). In contrast, MT significantly reduced BWG in MT-PCO when compared to PCO and the control group, $p = 0.000$ (Table 1).

Light microscopic results

H&E results

Control ovarian cortex showed many follicles at different stages of development; unilayer primary follicles, multilayer primary follicles and secondary follicles with few stromal interstitial cells. An antral follicle showed granulosa cells, an oocyte with corona radiata and many layers of cumulus oophoros. Mature graffian follicles with large cavities filled with liquor folliculi and surrounded with theca interna and theca externa cells were also observed (Fig. 1A & 1B). A corpus luteum with an outer layer of theca lutein cells and inner granulosa cells was seen (Fig. 1C).

In the PCO group, the cortex showed many follicular cysts of different shape and wall thickness that contained acidophilic materials in their lumens and were separated by highly cellular interstitial stroma (Fig. 2A). Higher magnifications

showed thick walled follicular cysts formed mainly of theca interna cells. Some cysts were folded, of thin walls and formed of one layer of granulosa cells surrounded by a thick layer of theca cells (Fig. 2B). Many follicles with no oocytes and numerous congested blood vessels in between were observed (Fig. 2C). Large cystic antral follicles filled with amorphous liquor folliculi showed degenerated granulosa cells and thick layered theca cells with signs of luteinization (Fig. 2D).

On the other hand, MT-PCO rats showed nearly normal ovarian cortex with many follicles in different stages of development, multilayer primary follicles and secondary follicles with oocyte in lumen. A small amount of interstitial stroma was observed when compared to that of PCO (Fig. 3A). Many growing and secondary follicles with thick walls formed of many layers of granulosa cells, theca interna and theca externa layers, containing oocytes surrounded by zona pellucida, in addition to a low level of stroma were seen (Fig. 3B). Corpora lutea with small lipid droplets in their granulosa and theca lutein cells and one growing follicle with some vacuolations of its follicular cell were also seen (Fig. 3C).

Immunohistochemical results

Anti VEGF-A immunostained section of control ovarian cortex showed a nearly negative immune reaction except for a mild positive reaction which

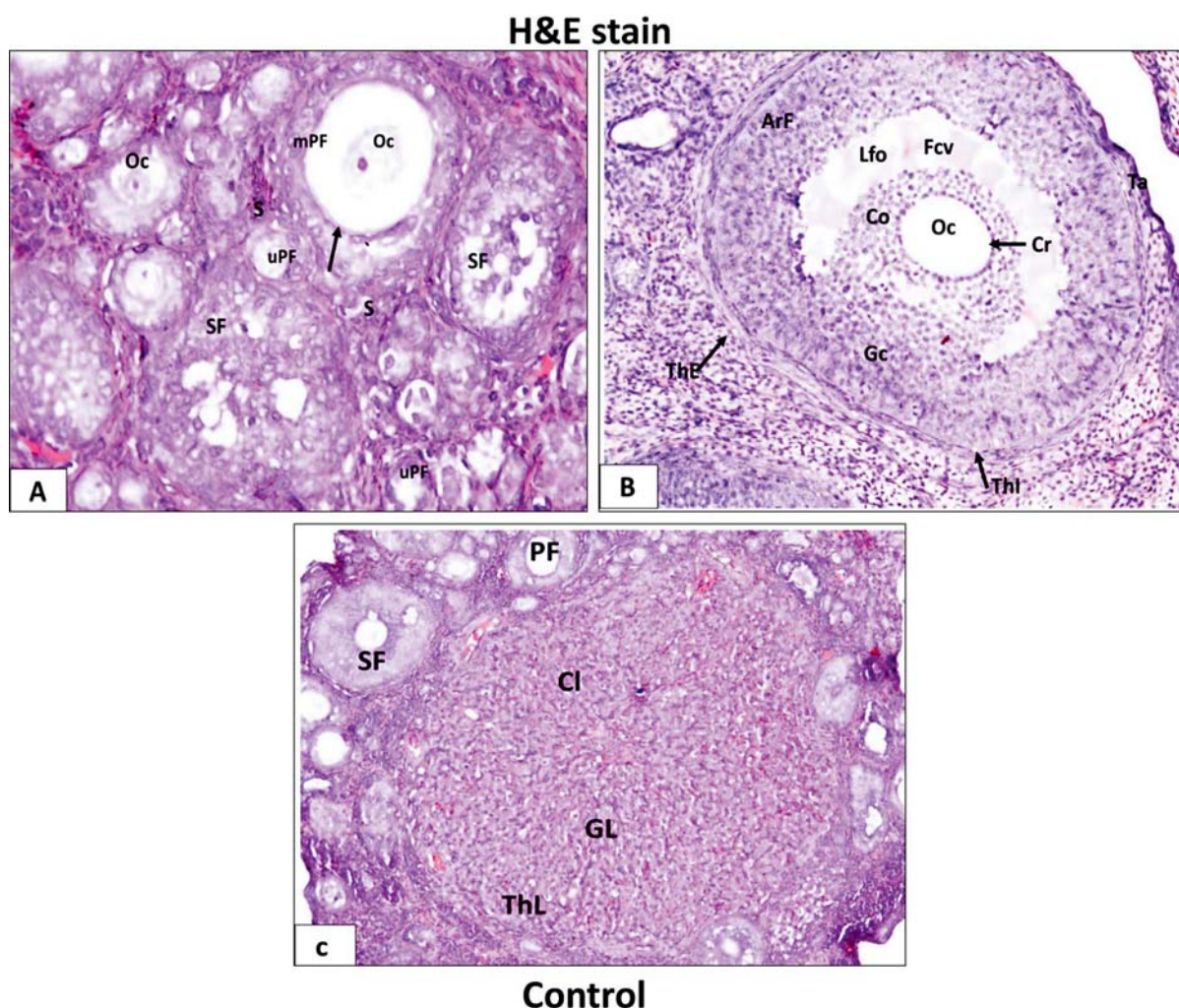


Fig.1. Photomicrography of control group H&E stained sections showing: A – Ovarian cortex with many follicles of different stages of development, unilayer primary follicles (uPF), multilayered primary follicles (mPF) and secondary follicles (SF). The follicles are separated by a few stromal interstitial cells (S). Some oocytes (Oc) appear in some follicles. B – An antral mature Graffian follicle (ArF) shows granulosa cells (Gc), an oocyte surrounded with corona radiata cells (Cr) and many layers of cumulus oophorus (Co). The follicle shows one large follicular cavity (Fcv) filled with liquor folliculi (Lfo) and surrounded by theca interna (ThI) and theca externa cells (ThE). C – A corpus luteum (CL) with outer layers of theca lutein cells (ThL) and inner granulosa cells (GL); secondary follicle (SF), primary follicle (PF). H&E stain; Ax400, B&Cx100.

was detected in the wall of blood vessels, by oocyte and liquor folliculi of some antral follicles (Fig. 4A). PCO rats exhibited strong positive VEGF-A immune reaction in the endothelial lining of the numerous blood vessels in the cortex, and medulla in addition to its appearance in granulosa cells of the follicles and its liquor fluid and some cells in the stroma (Fig. 4B). In MT-PCO rats, a positive VEGF-A immunoreaction was detected only in some blood vessels, top layer of granulosa cells and liquor folliculi (Fig. 4C).

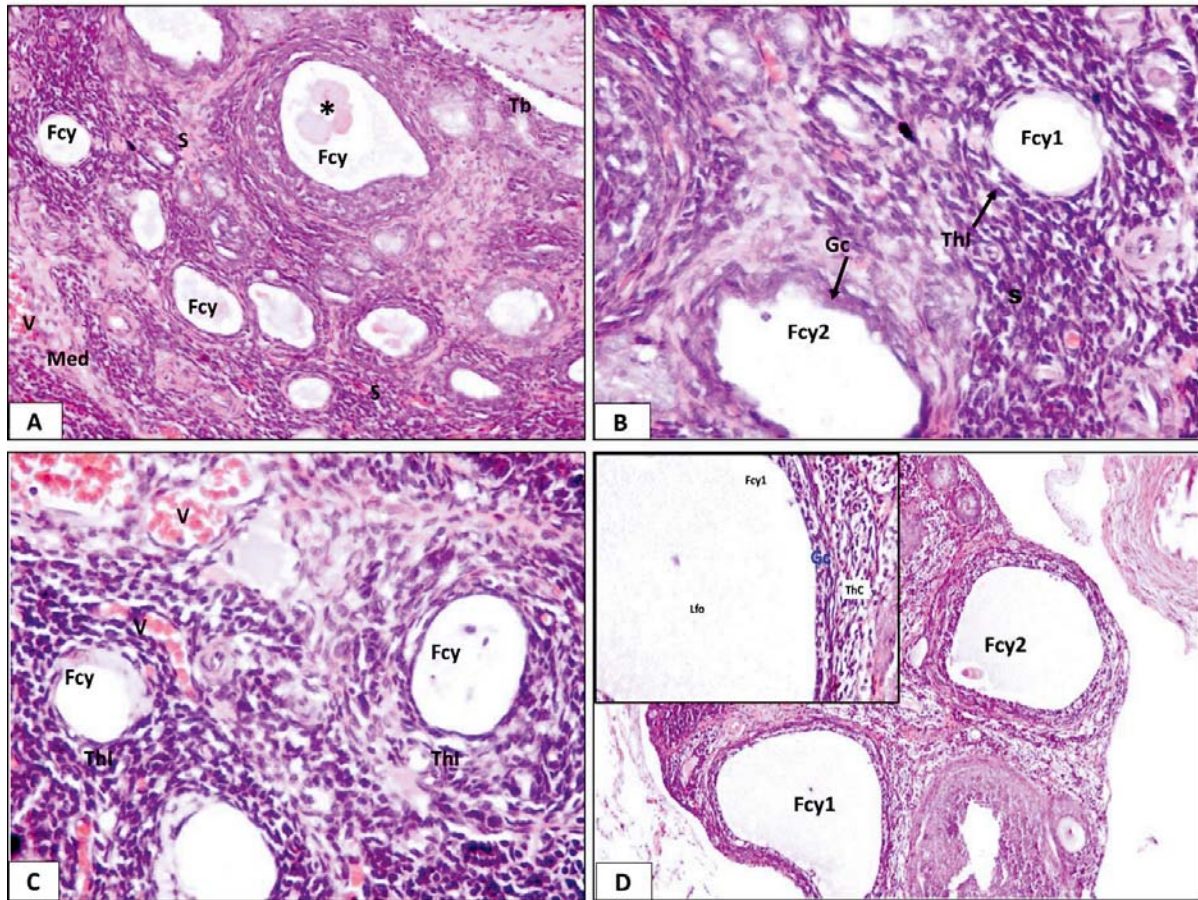
Anti-CTGF immunostained section of control ovaries showed weak CTGF immune reaction detected in follicles, endothelial cells of blood vessels and by few cells in the stroma (Fig. 5A). The PCO group exhibited strong positive CTGF im-

mune reaction which was detected by the majority of cells of the follicles, interstitial cells of the stroma and endothelial cells of the numerous blood vessels (Fig. 5B). An ovarian cyst with strong CTGF immune reaction exhibited in all layers was also detected (Fig. 5C). In MT-PCO, a positive CTGF immune reaction was detected only in the top cells of the granulosa layer of the follicle, some cells of corpus luteum and a few cells in the stroma (Fig. 5D).

Electron microscopic results

Electron micrographs of the control ovary showed a primordial follicle with an oocyte and a single layer of flat follicular cells, and multilayer primary follicles formed of two layers of follicular cells, both follicles were surrounded by intact

H&E stain



PCO

Fig. 2. Photomicrography of PCO group H&E stained sections showing: A – Cortex with many follicular cysts (Fcy) of different shape and wall thickness that contain acidophilic materials (stars) in their lumens and are separated by highly cellular interstitial stroma (S). B – Higher magnification of the previous figure showing two follicular cysts; The wall of one cyst (Fcy1) is thick and formed mainly of theca interna cells (ThI) and the wall of another cyst (Fcy2) is folded, thin and formed of one layer of granulosa cells surrounded by a thick layer of theca cells. C – Many follicular cysts (Fcy) with no oocytes that have thick walls formed mainly of theca interna cells. Note the numerous congested blood vessels (V) in the cortex. D – Two large cystic antral follicles (Fcy1&Fcy2). Inset: higher magnification of Fcy1 shows that it has thin walls which are formed by a single layer of degenerated granulosa cells (Gc), surrounded by thick layers of theca cells (ThC) showing signs of luteinization and filled with amorphous liquor folliculi (Lfo); medulla (Med), blood vessel (V), tunica albugenia (Tb). H&E stain; Ax200, B&Cx400, Dx100.

basement membrane (Fig. 6A). The preantral follicle showed many layers of granulosa cells; the cells facing a cavity showed microvilli. Theca interna with elongated cells and euchromatic elongated nuclei and theca externa layer with elongated shape and more dense nuclei were seen surrounding the follicle (Fig. 6B).

The antral follicle showed large-sized granulosa cells with large euchromatic nuclei, numerous mitochondria, smooth endoplasmic reticulum and intact junction between them (Fig. 6C). Some interstitial stromal cells with no lipid droplets in their cytoplasm and blood vessel lined with endothelial cells were seen in the cortex (Fig. 6D). Corpus luteum with granulosa lutein cells with many lipid droplets was seen (Fig. 6E).

In PCO, a unilaminar primary follicle with a single layer of tall follicular cells which showed an irregular nucleus with areas of chromatin loss and cytoplasmic degeneration (Fig. 7A). A multilayer primary follicle formed of many layers of follicular cells with wide spaces between the cells was observed (Fig. 7B). A follicular cyst with a wall formed only of theca interna, containing many lipid droplets was seen. The lumen of the cyst contains degenerated granulosa cells and amorphous substances (Fig. 7C).

Additionally, another follicular cyst showed degenerated granulosa cells with small dense nuclei and many lipid droplets was found (Fig. 7D). The cortex showed hyperthecosis of theca interna cells with their luteinization, containing numerous lipid

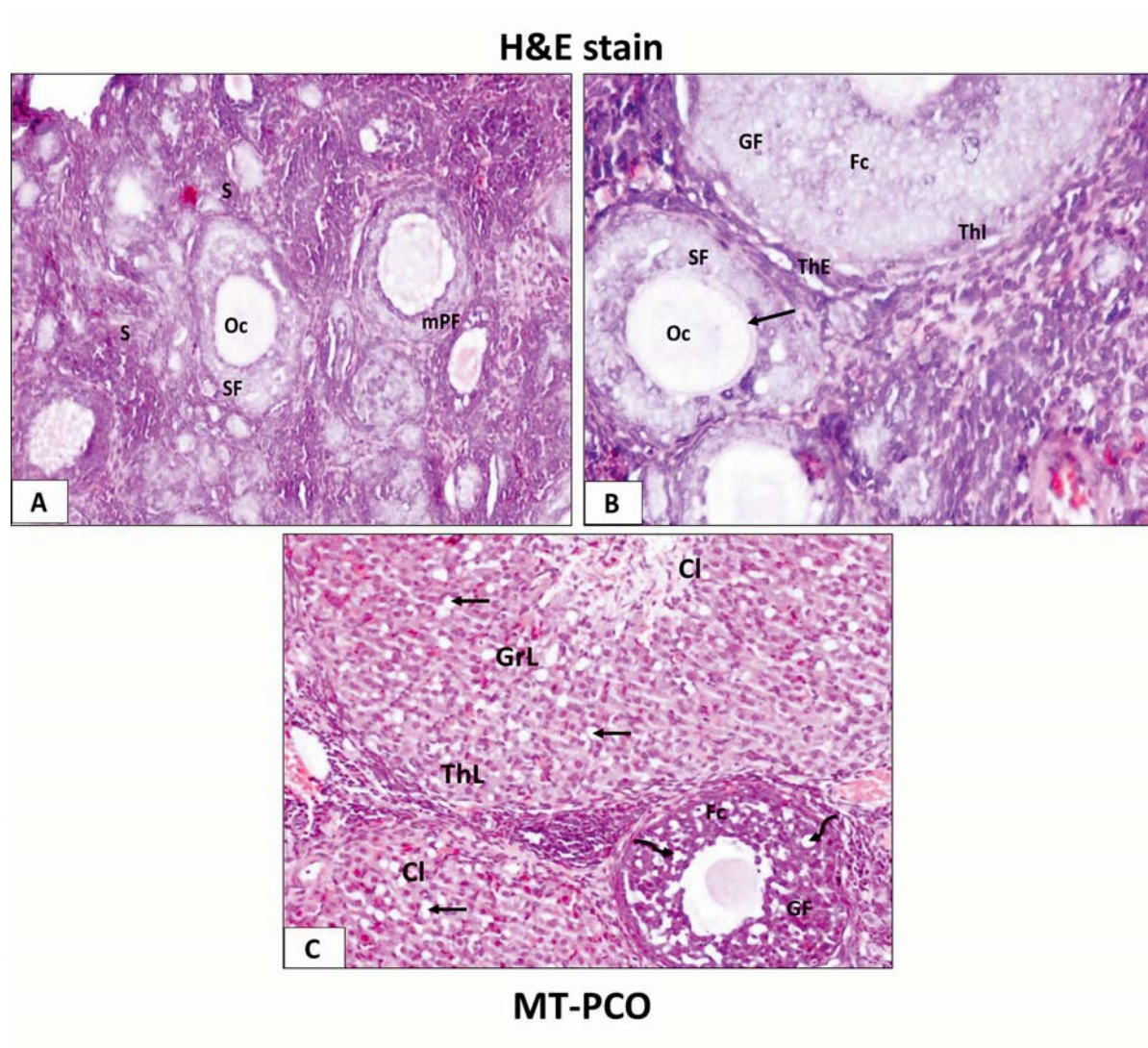


Fig. 3. Photomicrography of MT-PCO H&E stained section showing: A – nearly normal ovarian cortex with many follicles in different stages of development; multilayered primary follicles (mPF) and secondary follicles (SF) containing an oocyte (Oc) in its lumen. Note the little amount of interstitial stroma (S) when compared to that of PCO. B – Many growing (Gf) and secondary follicles. Both have thick walls formed of many layers of granulosa cells (Gc), theca interna (ThI) and theca externa layers (ThE). An oocyte (Oc) surrounded by zona pellucida (arrow) and little stroma (S) are seen. C – Two corpora lutea (CL) with small lipid droplets (arrows) in their granulosa (GL) and theca lutein (ThL) cells. One growing follicle (Gf) is apparent with some vacuolations (curved arrows) of its follicular cells (Fc). H&E stain; A&Bx400, Cx100.

droplets (Fig. 7E). In the medulla, some smooth muscle cells and one eosinophil with its characteristic ellipsoid granules were also observed (Fig. 7E).

In the MT-PCO group, the ovary showed nearly normal features. A primordial follicle with an oocyte and a single layer of flat follicular cells was embedded in many interstitial stroma (Fig. 8A). Unilayer primary follicles with follicular cells; an oocyte and intact basement membrane were also observed (Fig. 8B). The preantral follicle showed many layers of granulosa cells, theca interna and theca externa layer (Fig. 8C). In the antral follicle large-sized granulosa cells with large euchromatic nuclei and numerous mitochondria were seen (Fig. 8D). Corpus luteum with granulosa lutein

cells containing numerous lipid droplets were also detected (Fig. 8E).

Morphometric results

A highly significant decrease in the mean number of primary, preantral, antral follicles and corpora lutea were detected when the PCO group was compared to the control group ($p = 0.000$). Cystic follicles were detected only in the PCO group (Table 2). When the MT-PCO group was compared to the PCO group, a highly significant increase in the mean number of primary, preantral, antral follicles and corpora lutea and a highly significant decrease in the mean number of cystic follicles were observed, $p = 0.000$ (Table 2).

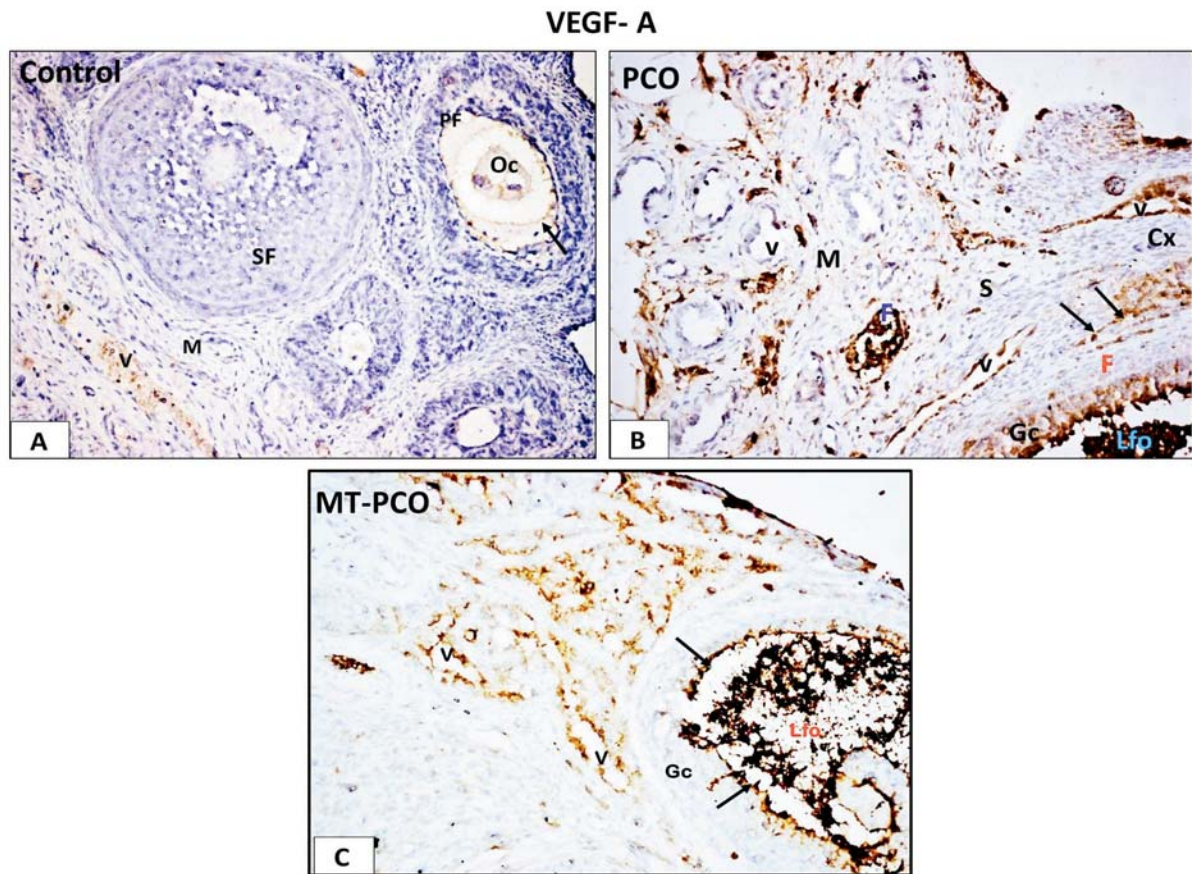


Fig. 4. Photomicrography of anti-VEGF-A immunostained sections: A – Control ovarian cortex shows nearly negative VEGF-A immune reaction except for a mild positive reaction in the wall of blood vessels (V), oocyte (Oc) and liquor folliculi (arrow) of some antral follicles (AF). B – PCO with strong positive VEGF-A immune reaction detected in the endothelial lining of the numerous blood vessels (V), cortex (Cx) and medulla (M), All layers of granulosa cells of the follicles (Gc), liquor fluid (Lof), and in some cells (arrows) in the stroma (S). C – MT-PCO shows positive VEGF-A immune reaction detected in many blood vessels (V), top layers only (arrows) of granulosa cells (Gc) and liquor folliculi cells (Flo). Anti-VEGF-A immunostain; Ax100; B x200 & Cx400.

Regarding the mean thickness of the granulosa cell layer of preantral and antral follicles, the PCO group showed a highly significant decrease when compared to the control group ($p = 0.000$) with the appearance of cystic follicles in the PCO group (mean thickness $11.87 \pm 0.43 \mu\text{m}$), while no cystic follicles were detected in the control group. On the other hand, a highly significant increase in the mean thickness of the theca interna cell layer was noticed in the PCO group when compared to the control group ($p = 0.000$) (Table 3). Compared to the PCO group, the mean thickness of the granulosa cell layer of preantral, antral and cystic follicles of MT-PCO rats showed a highly significant increase ($p = 0.000$), whereas the mean thickness of the theca interna cell layer showed a highly significant decrease, $p = 0.000$ (Table 3).

Regarding the mean area % of VEGF-A & CTGF-1 immunoexpression, a highly significant increase in both were detected when the PCO group (6.38 ± 0.19 and 8.33 ± 0.12) was compared to the

control group (1.06 ± 0.05 and 0.52 ± 0.03) respectively, $p = 0.000$, whereas a highly significant decrease was observed when the MT-PCO group (3.47 ± 0.11 and 4.17 ± 0.10) was compared to the PCO group, $p = 0.009$ (Fig. 9).

Discussion

PCOS is a composite and highly mixed disease characterized by insulin resistance, hyperandrogenism and obesity. Current management for PCOS patients involves the utilization of oral contraceptives, antiandrogens, and/or insulin sensitizers (LUQUE-RAMIREZ & ESCOBAR-MORREALE *et al.* 2010). Rodents are the most appropriate animal for PCOS models since they are plausibly priced, obtainable, have a short reproductive cycle, short estrous cycles, and a short gestational period. These PCOS models can be designed by giving hormones such as TP resulting in many fea-

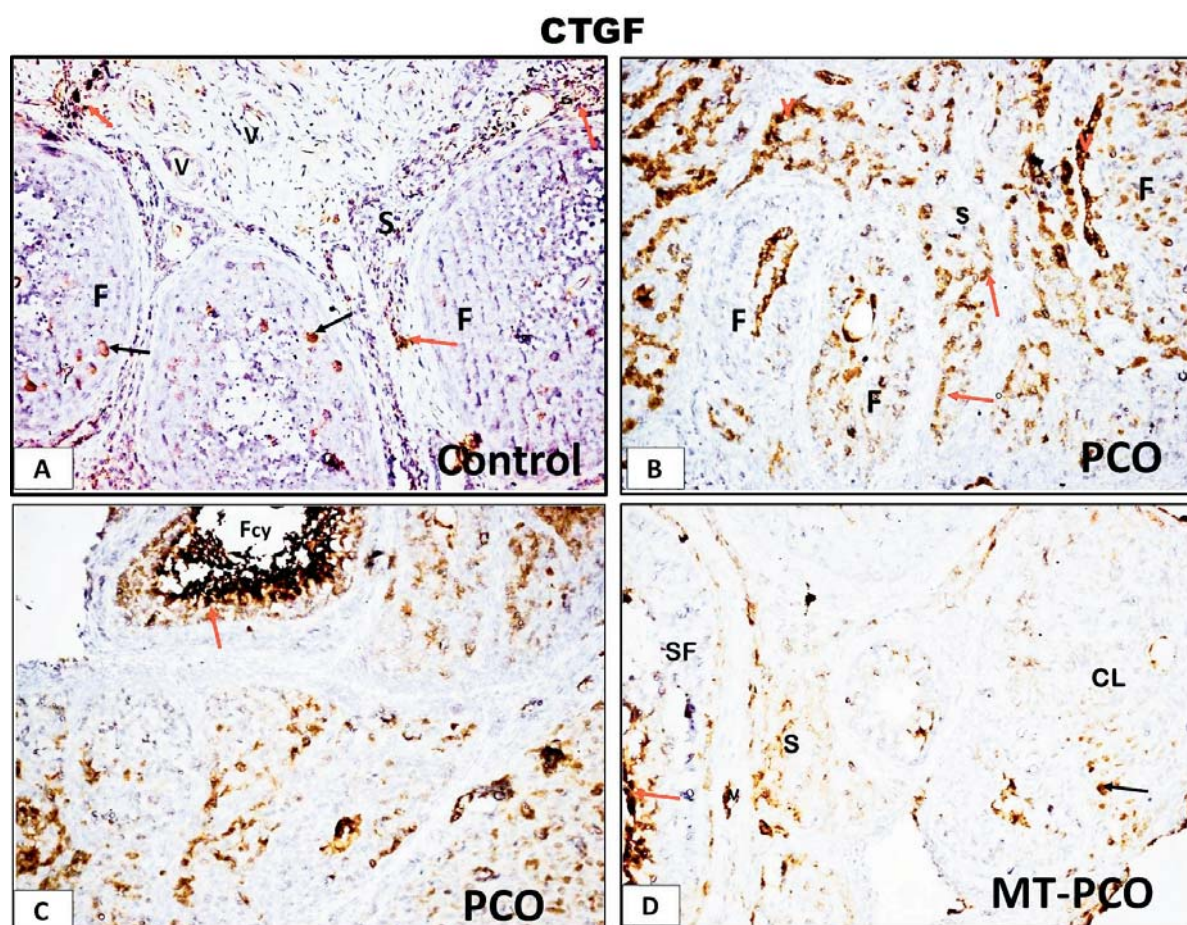


Fig. 5. Photomicrography of anti-CTGF immunostained sections: A – Control ovarian cortex shows weak CTGF immune reaction detected in some cells (black arrows) follicles (F), endothelial cells of blood vessels (V) and some cells (red arrows) in the stroma (S). B – PCO with strong positive CTGF immune reaction detected in most cells of the follicles (F), interstitial cells (arrows) of the stroma (S) and by the endothelial cells of numerous blood vessels (V). C – PCO with an ovarian cyst (Fcy) with strong CTGF immunoreaction exhibited in all layers (arrow) of the cyst. D – MT-PCO shows mild positive CTGF immune reaction detected in some cells (red arrows) of granulosa layer of a secondary follicle (SF), some cells (black arrow) of corpus luteum (CL) and few cells in the stroma (S). Anti-CTGF immunostain; A x200; B x200, C & D x400.

tures of typical human PCOS (WALTERS *et al.* 2012; PADMANABHAN & VEIGA-LOPEZ *et al.* 2013). Treatment of 3 week old rats with TP induced anovulation increased the incidence of apoptotic follicles, unhealthy oocytes and insulin resistance (BELOOSESKY *et al.* 2004).

An increase in serum concentration of estrogen, testosterone and decreased progesterone hormone level, increased fasting insulin hormone, increased insulin resistance (significantly increased HOMA-IR) and decreased insulin sensitivity (significantly lowered QUICKI-IS) were noticed in PCO rats which is in agreement with many studies which suggested that β -cell dysfunction in the form of hyperinsulinemia and insulin resistances are features of PCOS (DUNAIF 1997). The modest hyperandrogenism characteristic of the PCO group may contribute to the associated IR in accordance with HURLIMAN *et al.* (2015). They reported that there

is an association between hyperandrogenism and IR. However, it remains unclear whether hyperandrogenism results from hyperinsulinemia and/or IR or vice versa in PCOS (DIAMANTI-KANDARAKIS *et al.* 2012).

IR was recognized in the current study by the increase in fasting blood glucose and elevated insulin levels. Insulin promotes GnRH & LH release and increases LH/FSH ratio thus altering ovarian steroid formation (DIAMANTI-KANDARAKIS 2008) leading to the arrest of follicular development resulting in chronic anovulation. Consequently, insulin synergizes with abnormally high LH to promote excess androgen production by ovarian theca cells and reduces hepatic sex hormone binding globulin synthesis, in that way causing hyperandrogenism (DUMESIC *et al.* 2015). It was proposed that testosterone could worsen insulin sensitivity as some enzymatic changes occur in the

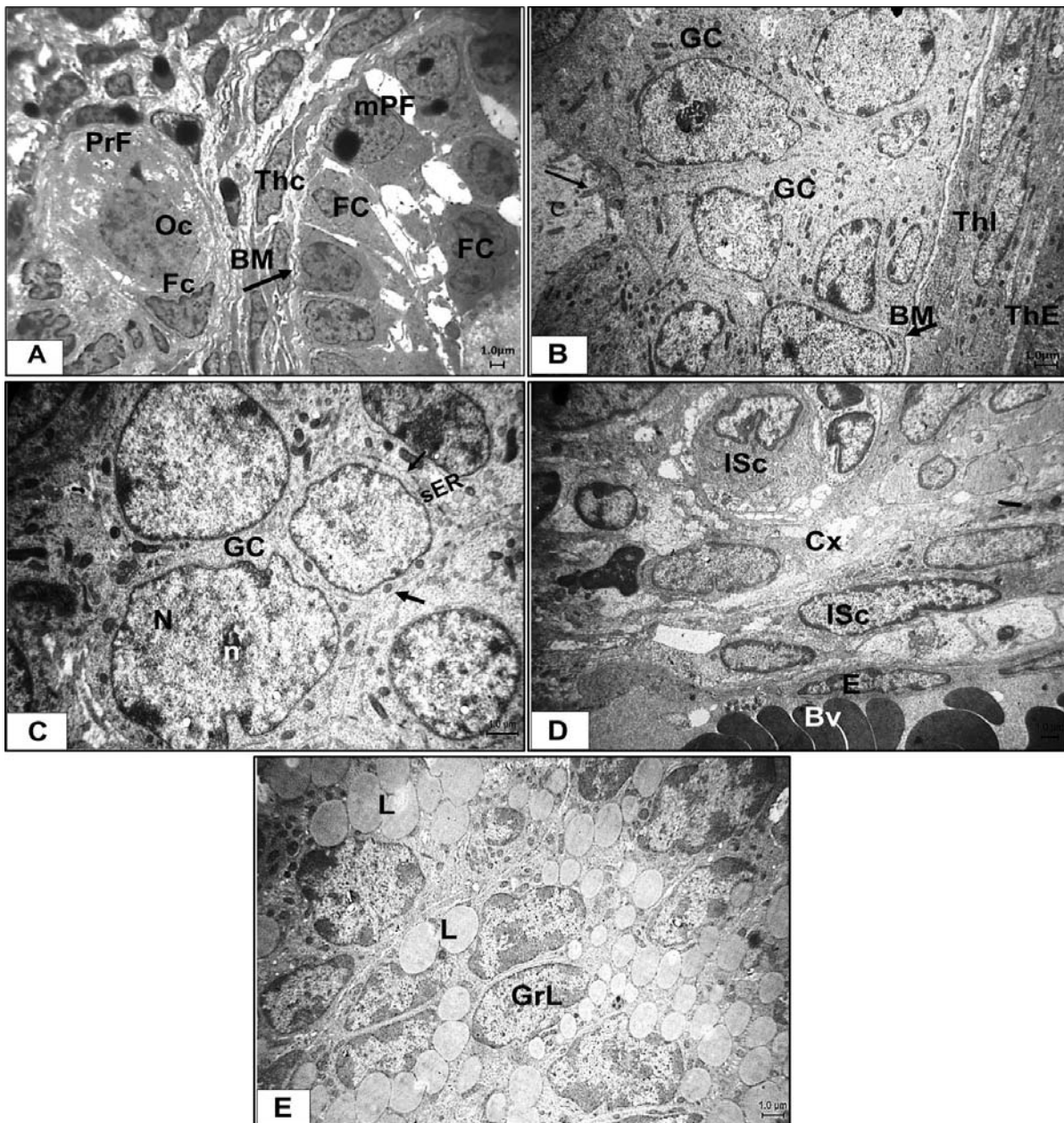


Fig. 6. An electron micrograph of the control ovary: A – Primordial follicle (PrF) contains an oocyte (Oc) and is surrounded by a single layer of flat follicular cells (FC) and multilayered primary follicles (mPF) formed of two layers of follicular cells (FC). Both follicles are surrounded by intact basement membrane (BM). B – Part of preantral follicle showing many layers of granulosa cells (GC); the cells facing a cavity (C) show microvilli (arrow). Theca interna (ThI) with characteristic elongated cells and euchromatic elongated nuclei and Theca externa layer (ThE) with elongated and more dense nuclei are seen surrounding the follicle. C – Part of antral follicle shows large sized granulosa cells (GC) with large euchromatic nuclei (N) containing nucleoli (n). The cells contain numerous mitochondria (m), smooth endoplasmic reticulum (sER) and show intact junctions (arrows) between them. D – Part of cortex (Cx) shows some interstitial stromal cells (IsC) with no lipid droplets in their cytoplasm and blood vessel (Bv) lined with endothelial cells (E). (E) Part of corpus luteum with granulosa lutein cells (GrL) which contain many lipid droplets (L). TEM, Ax2000, Bx4000, Cx6000, Dx3000 & Ex4000.

theca interna and interstitial cells ensuing in high levels of androgens and estradiol in PCO ovaries (LOMBARDI *et al.* 2014).

Other studies in testosterone-treated female rats have suggested that androgen-mediated insulin resistance may be a result of an increased number of less insulin-sensitive type II skeletal muscle fibers

(HOLMANG *et al.* 1992) and inhibition of muscle glycogen synthase activity (MANNERÅS *et al.* 2007). Furthermore, it was found that IR in at least 50% of PCOS women appeared to be related to excessive serine phosphorylation of the insulin receptor. Such phosphorylation modulates the activity of the key regulatory enzyme of androgen biosynthesis, P450c17. It is possible that this single defect in P450c17 may

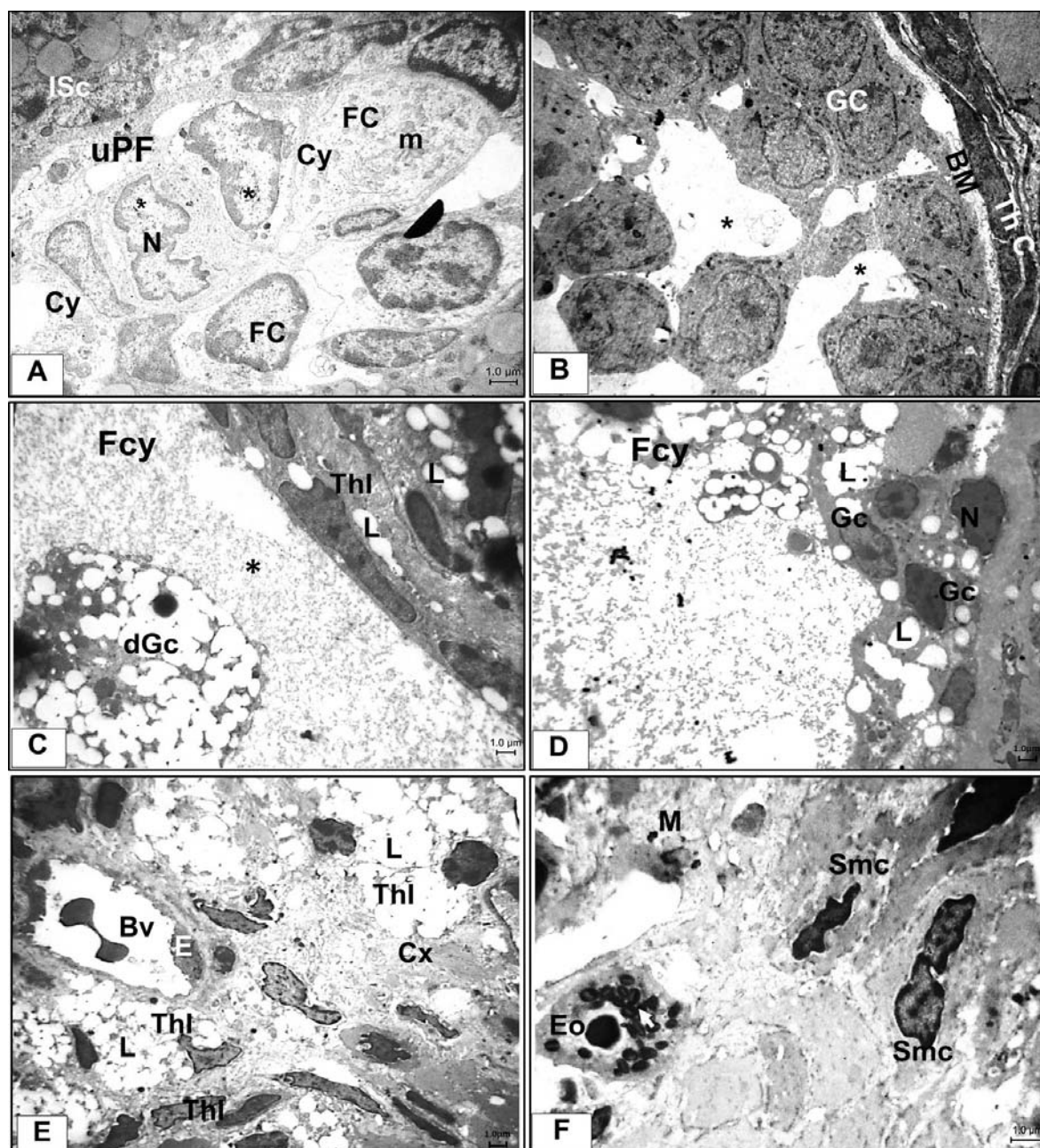


Fig. 7. An electron micrograph of the PCO group: A – Unilaminar primary follicle (uPF) with a single layer of tall follicular cells (FC) which shows an irregular nucleus (N) with areas of chromatin loss (stars) and cytoplasmic degeneration (Cy). B – Part of multilayer primary follicles (mPF) formed of many layers of follicular cells (FC) with wide spaces between the cells (stars). Note the basement membrane (BM), theca cells (ThC). C – Part of follicular cyst (Fcy) shows that the wall is formed only of theca interna (ThI) which contain many lipid droplets (L). The lumen of the cyst contains degenerated granulosa cells (dGc) and amorphous substances (star). D – Part of the follicular cyst (Fcy) shows that the wall is formed of degenerated granulosa cells (Gc) with substance small nuclei (N) and many lipid droplets (L). E – Part of the cortex (Cx) shows hyperthecosis of theca interna (ThI) cells with their luteinization, containing numerous lipid droplets (L). Note a blood vessel (Bv) with endothelial cells (E). F – Part of medulla (M) with some smooth muscles (Smc) and one eosinophil cell (Eo) is shown with its characteristic ellipsoid granules (white arrow). TEM, Ax4000; B, C, D & Ex3000; Fx6000.

produce both insulin resistance and hyperandrogenism in some PCOS women (BREMER & MILLER 2008; DIAMANTI-KANDARAKIS *et al.* 2012).

In the current work, a decrease in estrogen, testosterone and fasting insulin hormones and an increase in progesterone hormone levels were detected. In addition, a decrease in HOMA-IR and an

increase in QUICKI-IS were detected in MT treated rats. Previous work supports our results by evaluating the effect of MT treatment on patient with PCO, where a reduction on the circulating testosterone, Δ -4-androstenedione and hirsutism score were observed (MAZZA *et al.* 2014). Another similar study reported that MT treatment significantly inhibited fasting insulin and HOMA-IR in

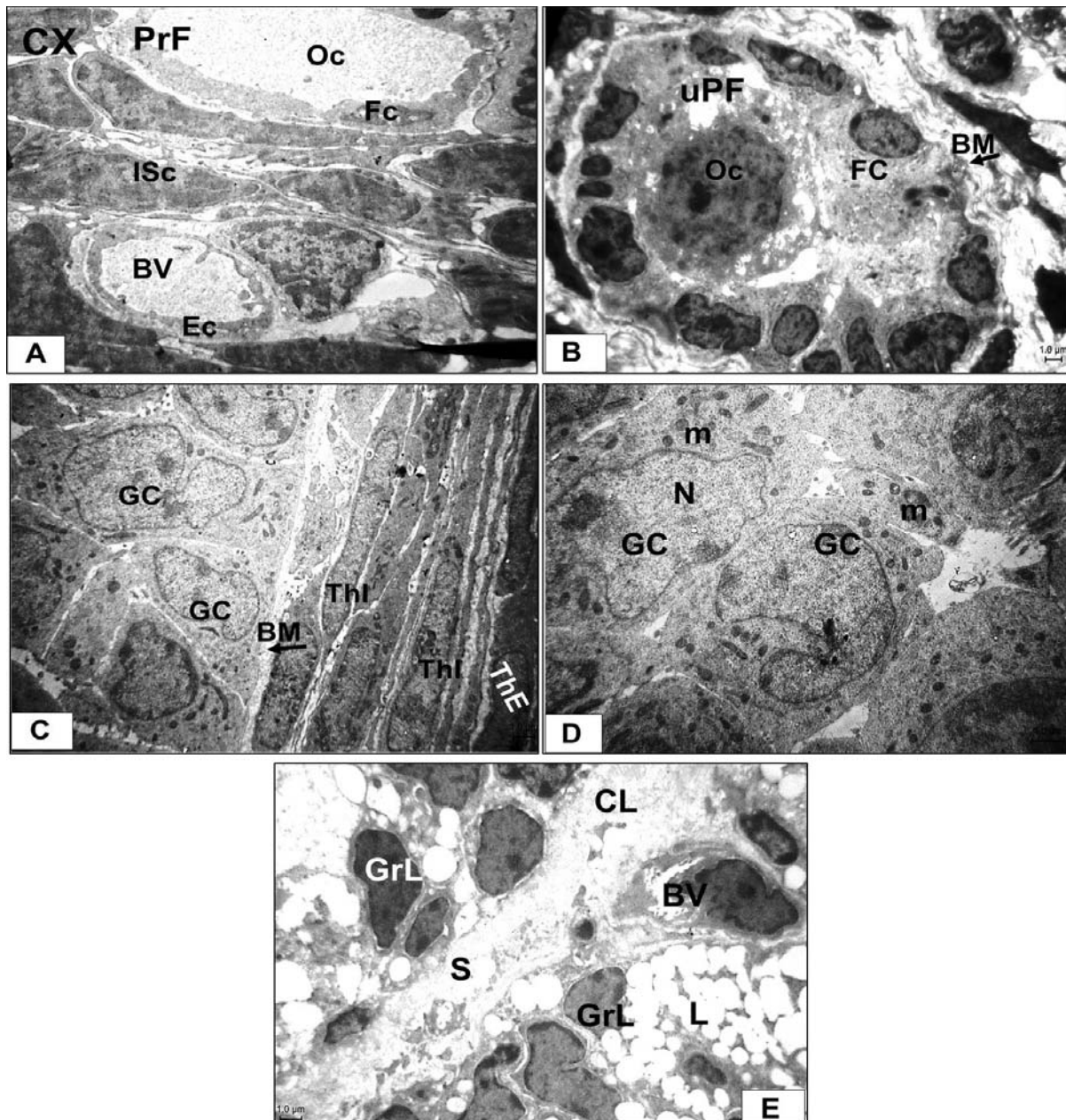


Fig. 8. An electron micrograph of the MT-PCO group; A – Primordial follicle (PrF) contains an oocyte (Oc) and is surrounded by a single layer of flat follicular cells (Fc) embedded in many interstitial stromal cells (ISc) and a blood vessel (BV) lined with endothelial cells (E) is present in the cortex (CX). B – Unilayer primary follicles (uPF) with follicular cells (FC), an oocyte (Oc) and intact basement membrane (BM). C – Part of preantral follicle shows many layers of granulosa cells (GC); theca interna (ThI) and theca externa layer (ThE). D – Part of antral follicle shows large sized granulosa cells (GC) with large euchromatic nuclei (N) with numerous mitochondria (m). E – Part of corpus luteum (CL) with granulosa lutein cells (GrL) containing many lipid droplets (L). Note: blood vessel (BV) in the CT septa (S) of the CL. TEM, A & B x3000, Cx4000, Dx6000, Ex4000.

PCOS rats (WU *et al.* 2018). As well, MT augmented the tyrosine kinase action of insulin receptors through alteration of plasma cell differentiation antigen. Also, it improves IS, lower serum LH, free and total testosterone concentration and causes elevation in FSH and sex hormone binding (SANGRAULA *et al.* 2009). Therefore, it is suggested that restoration of androgen and insulin levels and reduction of IR by MT could contribute in maintaining normal ovulatory function.

In the current study, an increase in the body weight and subsequent obesity was apparent in PCO rats. EHRMANN (2005) reported that obesity is intimately linked with PCOS where its percentage may involve up to 75% of patients. PCOS women have many risk factors of dyslipidemia with hyper triacylglycerolemia, reduced HDL and increased LDL when compared to normal BMI women (BERNEIS *et al.* 2007). It was confirmed that obesity played a chief role in the pathophysiol-

Table 2

Mean number of primordial, primary, preantral, antral and cystic follicles and corpus luteum in control, PCO and MT-PCO groups. Data are represented as mean \pm standard error of mean (SEM). N=30 measurements/group

Group	Primordial	Primary	Preantral	Antral	Cystic	Corpus luteum
Control	46.20 \pm 0.85	16.00 \pm 0.44	6.93 \pm 0.25	3.70 \pm 0.26	0.00	3.97 \pm 0.23
PCO p1	43.03 \pm 0.73 0.000	7.67 \pm 0.40 0.000	3.07 \pm 0.22 0.000	2.17 \pm 0.16 0.000	4.13 \pm 0.27 0.000	0.60 \pm 0.11 0.000
MT-PCO p2 p3	44.13 \pm 0.83 0.000 0.000	13.90 \pm 0.53 0.000 0.000	5.57 \pm 0.27 0.000 0.000	3.40 \pm 0.20 0.000 0.000	1.33 \pm 0.12 0.000 0.000	2.60 \pm 0.18 0.000 0.000

p: Probability

p1: significance between control and PCO groups.

p2: significance between PCO and MT-PCO groups.

p3: significance between control and MT-PCO groups.

Table 3

Mean thickness (μ m) of granulosa (Gc) and theca interna cells (ThI) of preantral, antral and cystic follicles in control, PCO and MT-PCO groups. Values are represented as mean \pm standard error of mean (SEM). N=30 measurements/measured parameter/group

Group/parameter	Preantral follicle	Antral follicle	Cystic follicle
Control Gc ThI	55.40 \pm 1.06 15.67 \pm 0.26	50.20 \pm 0.82 14.77 \pm 0.23	0.00 0.00
PCO Gc ThI p1a p1b	36.70 \pm 0.81 22.40 \pm 0.60 0.000 0.000	28.43 \pm 0.87 33.13 \pm 0.83 0.000 0.000	11.87 \pm 0.43 42.03 \pm 0.85 0.000 0.000
MT-PCO Gc ThI p2a p2b p3a p3b	47.03 \pm 0.98 18.30 \pm 0.39 0.000 0.000 0.000 0.000	45.40 \pm 1.07 20.20 \pm 0.49 0.000 0.000 0.000 0.000	24.03 \pm 0.60 27.97 \pm 0.89 0.000 0.000 0.000 0.000

p: Probability

a: significance when comparing Gc thickness between groups.

b: significance when comparing ThI thickness between groups.

p1: significance between control and PCO groups

p2: significance between PCO and MT-PCO groups.

p3: significance between control and MT-PCO groups.

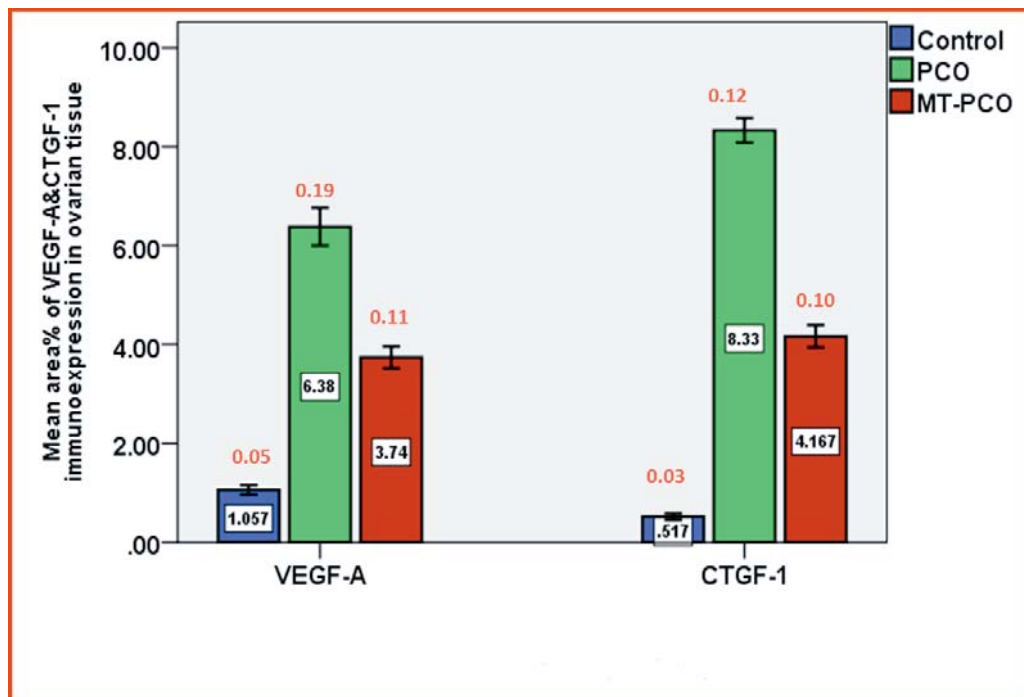


Fig. 9. Clustered bars representing the mean area % of VEGF-A & CTGF-1 immunoreactivity in ovarian tissue of Control, PCO & MT-PCO groups. Both VEGF-A & CTGF-1 show a highly significant increase when PCO group is compared to control and a decrease when it is compared to MT-PCO groups, $p \leq 0.001^{***}$ between the groups. Values are expressed as mean \pm standard error of mean (SEM) (red colored values).

ogy of hyperandrogenism and chronic anovulation yet, the etiology of obesity in such cases was not understandable since a nasty cycle of IR, abdominal fatness and hyperandrogenemia were proposed (VRBIKOVA & HAINER 2009). The recognized decrease in the body weight in MT treated rats in the present work raises the effectiveness of MT in reduction of obesity in PCO. Our results are in agreement with GHANDI *et al.* (2011) and AGARWAL *et al.* (2010) who found that treatment with MT caused a significant reduction in body weight, BMI and waist circumference. In summary, significantly decreased BWG to the normal value in the MT-PCO group compared to the PCO group might provide another explanation to the lowered testosterone level in this group, since weight loss is well known to decrease androgen levels and restore ovulation in PCOS (APTER 1998). Therefore, we suggest that a reduction in circulating insulin levels by MT might be one of the mechanisms for weight reduction-related reproductive paybacks.

PCO was also recognized by the appearance of large, thick walled follicular cysts with no oocytes, degenerated granulosa cells and thick theca cell layer. Additionally, TEM examination revealed that the follicular cells had irregular nuclei with areas of chromatin loss and cytoplasmic degeneration. Moreover, granulosa cells had dense small nuclei with hyperthecosis of theca cells containing many lipid droplets as previously described by CHANG (2007), LOMBARDI *et al.* (2014) and POORNIMA

et al. (2015). Statistically, a highly significant decrease in the mean number of all types of follicles, corpora lutea, mean thickness of granulosa cell layer was observed, whereas a highly significant increase in thickness of theca interna cells layer was further detected in this group. Such observations are in accordance with the findings of some former studies (MANNERÅS *et al.* 2007; KARIMZADEH *et al.* 2013; SUN *et al.* 2013). The thickening of theca cell layer and accumulation of lipid within might reflect increased ovarian androgen synthesis which led to early follicular discrimination and conversion of the primordial follicles to primary ones. Also, this thickening reflects the addition of luteinized granulosa cells in the cyst wall rather than true hyperplasia (MANNERÅS *et al.* 2007). Raised androgen levels caused an increase in the adipocytes and disturbed both enzymes and proteins concerned in lipid metabolism (LOMBARDI *et al.* 2014).

MT treatment improved the histological and ultrastructural picture of the ovary which was supported by a detection of an increase in the number of all types of follicles, corpora lutea, thickness of granulosa cells and decrease in the number of follicular cysts and thickness of theca interna of mature follicles. MT was proved to cause a diminution in the completion of meiosis 1 by mouse oocytes *in vitro* and an increase in the liberation of mature oocytes and their total number *in vivo* (SABATINI *et al.* 2011). Previous data verified an antiapoptotic effect of MT on luteinized granulosa

cells in PCOS patients undergoing IVF (ONALAN *et al.* 2005). Furthermore, MT caused improvement of oxidative stress, endothelial dysfunction (KOCER *et al.* 2014) and numerous inflammatory markers (DIAMANTI-KANDARAKIS *et al.* 2006). Also, adding MT to the ovarian stimulation procedure in PCOS women reduced the risk of ovarian hyperstimulation syndrome, incidence of early pregnancy loss and gestational diabetes (SANGRAULA *et al.* 2009; TSO *et al.* 2009). MT improved the action of insulin on oocyte glutathione (GSH) content which drives out the free radicals from the oocytes resulting in better oocyte proficiency (MOTTA 2010).

The PCO group in the current work showed strong positive immune reaction for VEGF while in the MT-PCO group; this immunoreactivity was limited to some blood vessels, top cells of granulosa layer and few stromal cells. These data were consistent with the works of PEITSIDIS and AGRAWAL (2010) and MIAO *et al.* (2012). Previous studies found an increase in the number and volume of blood vessels in the theca interna and medulla of ovaries in PCO rats as shown in the current work. VEGF is a key regulator of angiogenesis and controls the proliferation, migration, differentiation, and survival of endothelial cells (STAHMANN *et al.* 2010). Another report detected significant augmentation of the vascular diameter in PCO model mice than controls (ZHOU *et al.* 2008). In PCOS, hyperandrogenism and hyperglycemia may be capable of promoting inflammation resulting in generation of reactive oxygen species (ROS) from peripheral blood mononuclear cells and subsequently increases in IL-6, COX-2 and VEGF. The increase in the thickness of follicular theca and the ovarian stroma volume may be due to neoangiogenesis and VEGF expression in the ovary (BARAVALLE *et al.* 2006). These observations indicate that in addition to formation of follicular cysts, increased vascularity could be a characteristic feature of PCO syndrome. Anti-VEGF therapy has been demonstrated to be useful in the treatment of pathological angiogenesis. Many prior clinical studies confirmed that diabetic patients treated with MT were unlikely to have vascular complications. Furthermore, it has a remarkable potential to treat vascular dysfunction and tumor angiogenesis in conditions other than diabetes. MT alleviated the diabetic retinopathy apparently throughout attenuating retinal and choroidal neovascularization by inhibition of VEGF signaling (KANNARKATT *et al.* 2016; YI *et al.* 2016). Once more, MT triggered AMP-activated protein kinase (AMPK) which mediates regulation of angiogenesis and endothelial cell function (TAKEUCHI *et al.* 2013). Surprisingly, it inhibited endothelial progenitor cell angiogenesis

through stoppage of the autophagy pathway (MA *et al.* 2017).

Our results showed strong CTGF expression by ovarian follicles and interstitial connective tissue stroma in the PCO group and their decrease in the MT-PCO group. Ovarian follicular development involves uninterrupted modification of the extracellular matrix to form the basement membrane and intercellular framework so as to maintain growth and differentiation of granulosa cells. It could be that ovarian fibrosis results from the degeneration of granulosa cells, which causes interstitial hyperplasia and collagen deposition. PCOS model in rats was a resource of profibrotic protein signaling such as TGF- β , CTGF and extracellular matrix (WANG *et al.* 2018). CTGF has an important role in collagen biosynthesis, cell motility and angiogenesis. Accordingly, overexpression of CTGF encourages fibrosis while its inhibition improves tissue repair and function (ZHOU *et al.* 2008; ZHANG *et al.* 2013; ZHOU *et al.* 2017).

Moreover, granulosa derived CTGF is the main stimulus for development and remodeling of theca cells (HARLOW *et al.* 2002). WANDJI *et al.* (2000) noted increased CTGF mRNA protein levels around vascular endothelial cells in pig ovarian follicles. ZHANG *et al.* (2013) detected increased expression of CTGF in the ovarian and uterine tissues of PCO rats compared to the controls which was attenuated by MT intake. MT has shown to be very efficient in reversing fibrosis by upregulating phosphorylated AMPK expression which attenuates ROS-induced oxidative stress (LEE *et al.* 2012; KUMAR *et al.* 2017). Interestingly, use of MT decreased the degree of lung damage and lowered the expression levels of the fibrosis markers and α -actin thus preventing bleomycin induced pulmonary fibrosis (LI *et al.* 2015). In addition, MT was also proved to significantly alleviate the lesions of hepatic steatosis and fibrosis, through marked reduction in the expressions of α -SMA and TGF β 1 in liver tissue of type 2 diabetic rats (QIANG *et al.* 2010). All these observations proved the role of CTGF in the occurrence of fibrosis in PCOS and function of MT as antifibrotic therapy.

Conclusion

From the present study, it can be concluded that increased insulin sensitivity, restoration of normal insulin, androgen levels and reduction of body weight in addition to the anti-angiogenic, antifibrotic effects of MT can improve histological, ultrastructural and associated hormonal changes in induced PCO in rats. Therefore, MT could be a promising treatment for PCOS associated infertility.

Author Contributions

Research concept and design: G.M.A.; Collection and/or assembly of data: G.M.A., R.A.E., M.H.E.; Data analysis and interpretation: G.M.A., R.A.E., M.H.E.; Writing the article: G.M.A., R.A.E., M.H.E.; Critical revision of the article: G.M.A., R.A.E.; Final approval of article: G.M.A.

Conflict of Interest

The authors declare no conflict of interest.

References

- AGARWAL N., RICE S.P.L., BOLUSANI H., LUZIO S.D., DUNSEATH G., LUDGATE M., REES D.A. 2010. *Metformin* reduces arterial stiffness and improves endothelial function in young women with polycystic ovary syndrome: a randomized, placebo-controlled, crossover trial. *J. Clin. Endocrinol. Metab.* **95**: 722-730. <https://doi.org/10.1210/jc.2009-1985>
- ALFARO M.P., DESKINS D.L., WALLUS M., DASGUPTA J., DAVIDSON J.M., NANNEY L.B.A., GUNEY A.M., GANNON M., YOUNG P.P. 2013. A physiological role for connective tissue growth factor in early wound healing. *Lab. Invest.* **93**: 81-95. <https://doi.org/10.1038/labinvest.2012.162>
- APTER D. 1998. How possible is the prevention of polycystic ovary syndrome development in adolescent patients with early onset of hyperandrogenism. *J. Endocrinol. Invest.* **21**: 613-617. <https://doi.org/10.1007/BF03350786>
- BANCROFT A.D., GAMBLE M. 2008. *Theory and Practice of Histological Techniques*. 6th ed. Philadelphia: Churchill Livingstone/Elsevier.
- BARAVALLE C., SALVETTI N., MIRA G., PEZZONE N., ORTEGA H. 2006. Microscopic characterization of follicular structure in letrosole-induced polycystic ovarian syndrome in the rat. *Arch. Med. Res.* **37**: 830-839. <https://doi.org/10.1016/j.arcmed.2006.04.006>
- BARBER T.M., DIMITRIADIS G.K., ANDREOU A., FRANKS S. 2015. Polycystic ovary syndrome: insight into pathogenesis and a common association with insulin resistance. *Clin. Med.* **15**: s72-s76. <https://doi.org/10.7861/clinmedicine.15-6-s72>
- BARTHELMESS E.K., NAZ R.K. 2014. Polycystic ovary syndrome: current status and future perspective. *Front. Biosci.* **6**: 104-119.
- BELOOESKY R., GOLD R., ALMOG B., SASSON R., DANTES A., LAND-BRACHA A., HIRSH L., ITSKOVITZ-ELDOR J., LESSING J.B., HOMBURG R., AMSTERDAM A. 2004. Induction of polycystic ovary by testosterone in immature female rats: Modulation of apoptosis and attenuation of glucose/insulin ratio. *Int. J. Mol. Med.* **14**: 207-215. <https://doi.org/10.3892/ijmm.14.2.207>
- BERNEIS K., RIZZO M., LAZZARONI V., FRUZZETTI F., CARMINA E. 2007. Atherogenic lipoprotein phenotype and low density lipoproteins size and subclasses in women with polycystic ovary syndrome. *J. Clin. Endocrinol. Metab.* **92**: 186-189. <https://doi.org/10.1210/jc.2006-1705>
- BREMER A.A., MILLER W.L. 2008. The serine phosphorylation hypothesis of polycystic ovary syndrome: a unifying mechanism for hyperandrogenemia and insulin resistance. *Fertil. Steril.* **89**: 1039-1048. <https://doi.org/10.1016/j.fertnstert.2008.02.091>
- CARMINA E., OBERFIELD S.E., LOBO R.A. 2010. The diagnosis of polycystic ovary syndrome in adolescents. *Am. J. Obstet. Gynecol.* **203**: 201.e1-201.e5. <https://doi.org/10.1016/j.ajog.2010.03.008>
- CHANG R.J. 2007. The reproductive phenotype in polycystic ovary syndrome. *Nat. Clin. Pract. Endocrinol. Metab.* **3**: 688-695. <https://doi.org/10.1038/ncpendmet0637>
- DIAMANTI-KANDARAKIS E., PATERAKIS T., KANDARAKIS H.A. 2006. Indices of low-grade inflammation in polycystic ovary syndrome. *Ann. N. Y. Acad. Sci.* **1092**: 175-186. <https://doi.org/10.1196/annals.1365.015>
- DIAMANTI-KANDARAKIS E. 2008. Polycystic ovarian syndrome: pathophysiology, molecular aspects and clinical implications. *Expert. Rev. Mol. Med.* **10**: e3. <https://doi.org/10.1017/S1462399408000598>
- DIAMANTI-KANDARAKIS E., SPRITZER P.M., SIR-PETERMANN T., MOTTA A.B. 2012. Insulin resistance and polycystic ovary syndrome through life. *Curr. Pharm. Des.* **18**: 5569-5576.
- DUMESIC D.A., LOBO R.A. 2013. Cancer risk and PCOS. *Steroids* **78**: 782-785. <https://doi.org/10.1016/j.steroids.2013.04.004>
- DUMESIC D.A., OBERFIELD S.E., STENER-VICTORIN E., MARSHALL J.C., LAVEN J.S., LEGRO R.S. 2015. Scientific Statement on the Diagnostic Criteria, Epidemiology, Pathophysiology, and Molecular Genetics of Polycystic Ovary Syndrome. *Endocr. Rev.* **36**: 487-525. <https://doi.org/10.1210/er.2015-1018>
- DUNAIF A. 1997. Insulin Resistance and the Polycystic Ovary Syndrome: Mechanism and Implications for Pathogenesis. *Endocr. Rev.* **18**: 774-800. <https://doi.org/10.1210/edrv.18.6.0318>
- EHRMANN D.A. 2005. Polycystic ovary syndrome. *N. Eng. J. Med.* **352**: 1223-1236. <https://doi.org/10.1056/NEJMra041536>
- GAMBINERI A., PELUSI C., VICENNATI V., PAGOTTO U., PASQUALI R. 2002. Obesity and the polycystic ovary syndrome. *Int. J. Obes. Relat. Metab. Disord.* **26**: 883-896. <https://doi.org/10.1038/sj.ijo.0801994>
- GHANDI S., AFLATOONIAN A., TABIBNEJAD N., MOGHADAM M.H.S. 2011. The effects of metformine or orlistat on obese women with polycystic ovary syndrome: a prospective randomized open-label study. *J. Assist. Reprod. Genet.* **28**: 591-596. <https://doi.org/10.1007/s10815-011-9564-2>
- GLAURET A.M., LEWIS P.R. 1998. *Biological Specimen Preparation for Transmission Electron Microscopy*. 1st ed. London, Portland Press. Pp.326.
- GOODMAN N.F., COBIN R.H., FUTTERWEIT W., GLUECK J.S., LEGRO R.S., CARMINA E. 2015. American association of clinical endocrinologists, American college of endocrinology and androgen excess and PCOS society disease state clinical review: guide to the best practices in the evaluation and treatment of polycystic ovary syndrome – part 1. *Endocr. Pract.* **21**: 1291-1300. <https://doi.org/10.4158/EP15748.DSC>
- HARLOW C.R., DAVIDSON L., BURNS K.H., YAN C., MATZUK M.M., HILLIER S.G. 2002. FSH and TGF- β 1 superfamily members regulate granulosa cell connective tissue growth factor gene expression *in vitro* and *in vivo*. *Endocrinology* **143**: 3316-3325. <https://doi.org/10.1210/en.2001-211389>
- HOLMANG A., LARSSON B.M., BRZEZINSKA Z., BJORNTORP P. 1992. Effects of short-term testosterone exposure on insulin sensitivity of muscles in female rats. *Am. J. Physiol.* **262**: E851-E855. <https://doi.org/10.1152/ajpendo.1992.262.6.E851>
- HSU S.M., RAINE L., FANGER H. 1981. Use of avidin-biotin-peroxidase complex (ABC) in immunoperoxidase techniques: a comparison between ABC and unlabeled antibody (PAP) procedures. *J. Histochem. Cytochem.* **29**: 577-580. <https://doi.org/10.1177/29.4.6166661>

- HURLIMAN A., BROWN K.J., MAILLE N., MANDALA M., CASSON P., OSOL G. 2015. Hyperandrogenism and insulin resistance, not changes in body weight, mediate the development of endothelial dysfunction in a female rat model of polycystic ovary syndrome (PCOS). *Endocrinology*. **156**: 4071-4080. <https://doi.org/10.1210/en.2015-1159>
- KANNARKATT J., ALKHARABSEH O., TOKALA H., DIMITROV N.V. 2016. Metformin and angiogenesis in cancer – revisited. *Oncology*. **91**: 179-184. <https://doi.org/10.1159/000448175>
- KARIMZADEH L., NABIUNI M., KOUCHESFEHANI H.M., ADHAM H., BAGHERI A., SHEIKHOLESLAMI A. 2013. Effect of bee venom on IL6, COX2 and VEGF levels in polycystic ovarian syndrome induced in Wistar rats by estradiol valerate. *J. Venom. Anim. Toxins. Incl. Trop. Dis.* **19**: 19-32. <https://doi.org/10.1186/1678-9199-19-32>
- KATZ A., NAMBI S.S., MATHER K., BARON A.D., FOLLMANN D.A., SULLIVAN G., QUON M.J. 2000. Quantitative insulin sensitivity check index: a simple, accurate method for assessing insulin sensitivity in humans. *J. Clin. Endocrinol. Metab.* **85**: 2402-2410. <https://doi.org/10.1210/jcem.85.7.6661>
- KJØTRØD S.B., CARLSEN S.M., RASMUSSEN P.E., HOLST-LARSEN T., MELLEBAKKEN J., THURIN-KJELLBERG A., HAAPANIEMI K., MORIN-PAPUNEN L., HUMAIDAN P., SUNDE A., VON DÜRING V. 2011. Use of Metformin before and during assisted reproductive technology in non-obese young infertile women with polycystic ovary syndrome: a prospective, randomized, double-blind, multi-centre study. *Hum. Reprod.* **26**: 2045-2053. <https://doi.org/10.1093/humrep/der154>
- KOCER D., BAYRAM F., DIRI H. 2014. The effects of Metformin on endothelial dysfunction, lipid metabolism and oxidative stress in women with polycystic ovary syndrome. *Gynecol. Endocrinol.* **30**: 367-371. <https://doi.org/10.3109/09513590.2014.887063>
- KUMAR S., KIM Y.R., VIKRAMA., NAQVIA., LI Q., KASSAN M., KUMAR V., BACHSCHMID M.M., JACOBS J.S., KUMAR A., IRANI K. 2017. Sirtuin1-regulated lysine acetylation of p66Shc governs diabetes-induced vascular oxidative stress and endothelial dysfunction. *PNAS*. **114**: 1714-1719. <https://doi.org/10.1073/pnas.1614112114>
- LAI K.B., SANDERSON J.E., YU C.M. 2013. The regulatory effect of norepinephrine on connective tissue growth factor (CTGF) and vascular endothelial growth factor (VEGF) expression in cultured cardiac fibroblasts. *Int. J. Cardiol.* **163**: 183-189. <https://doi.org/10.1016/j.ijcard.2011.06.003>
- LEE M.S., KIM S.H., KIM D.S., MIN K.S., YOON J.T. 2012. Metformin enhances the action of insulin on porcine granulosa-lutein cells in vitro. *Anim. Reprod. Sci.* **136**: 100-107. <https://doi.org/10.1016/j.anireprosci.2012.10.001>
- LI L., HUANG W., LI K., ZHANG K., LIN C., HAN R., LU C., WANG Y., CHEN H., SUN F., HE Y. 2015. Metformin attenuates gefitinib-induced exacerbation of pulmonary fibrosis by inhibition of TGF- β signaling pathway. *Oncotarget*. **6**: 43605-43619. <https://doi.org/10.18632/oncotarget.6186>
- LOMBARDI L.A., SIMÕES R.S., MAGANHIN C.C., BARACAT M.C., SILVA-SASSO G.R., FLORENCIO-SILVA R., SOARES J.M. Jr, BARACAT E.C. 2014. Immunohistochemical evaluation of proliferation, apoptosis and steroidogenic enzymes in the ovary of rats with polycystic ovary. *Rev. Assoc. Med. Bras.* **60**: 349-356.
- LUO J., LIANG Y., KONG F., QIU J., LIU X., CHEN A., LUXON B.A., WU H.W., WANG Y. 2017. Vascular endothelial growth factor promotes the activation of hepatic stellate cells in chronic schistosomiasis. *Immunol. Cell. Biol.* **95**: 399-407. <https://doi.org/10.1038/icb.2016.109>
- LUQUE-RAMIREZ M., ESCOBAR-MORREALE H.F. 2010. Treatment of polycystic ovary syndrome (PCOS) with Metformin ameliorates insulin resistance in parallel with the decrease of serum interleukin-6 concentrations. *Horm. Metab. Res.* **42**: 815-820. <https://doi.org/10.1055/s-0030-1262855>
- MA Y., LI W., LEI F., QIAN A., ZHU L., JIANG K., LI X. 2017. Metformin inhibits angiogenesis in endothelial progenitor cells through inhibiting MMP2, MMP9 and uPA expression via AMPK-mTOR-autophagy pathway. *Int. J. Clin. Exp. Med.* **10**: 958-964.
- MANNERÅS L., CAJANDER S., HOLMÅNG A., SELESKOVIC Z., LYSTIG T., LÖNN M., STENER-VICTORIN E. 2007. A New Rat Model Exhibiting both Ovarian and Metabolic Characteristics of Polycystic Ovary Syndrome. *Endocrinology*. **148**: 3781-3791. <https://doi.org/10.1210/en.2007-0168>
- MARCONDES F.K., BIANCHI F.J., TANNO A.P. 2002. Determination of the estrous cycle phases of rats: some helpful considerations. *Braz. J. Biol.* **62**: 609-614.
- MATTHEWS D.R., HOSKER J.P., RUDENSKI A.S., NAYLOR B.A., TREACHER D.F., TURNER R.C. 1985. Homeostasis model assessment: insulin resistance and β -cell function from fasting plasma glucose and insulin concentrations in man. *Diabetologia* **28**: 412-419.
- MAZZA A., FRUCI B., GUZZI P., D'ORRICO B., MALAGUARNERA R., VELTRI P., FAVA A., BELFIORE A. 2014. In PCOS patients the addition of low-dose spironolactone induces a more marked reduction of clinical and biochemical hyperandrogenism than metformin alone. *Nutr. Metab. Cardiovasc. Dis.* **24**: 132-139. <https://doi.org/10.1016/j.numecd.2013.04.016>
- MIAO Z.L., GUO L., WANG Y.X., CUI R., YANG N., HUANG M.Q., QIN W.B., CHEN J., LI H.M., WANG Z.N., WEI X.C. 2012. The Intervention Effect of Rosiglitazone in Ovarian Fibrosis of PCOS Rats. *Biomed. Environ. Sci.* **25**: 46-52. <https://doi.org/10.3967/0895-3988.2012.01.007>
- MOTTA A.B. 2010. Dehydroepiandrosterone to induce murine models for the study of polycystic ovary syndrome. *J. Steroid. Biochem. Mol. Biol.* **119**: 105-111. <https://doi.org/10.1016/j.jsbmb.2010.02.015>
- NORMAN R.J., DEWAILLY D., LEGRO R.S., HICKEY T.E. 2007. Polycystic ovary syndrome. *Lancet*. **370**: 685-697. [https://doi.org/10.1016/S0140-6736\(07\)61345-2](https://doi.org/10.1016/S0140-6736(07)61345-2)
- OLLILA M.E., WEST S., KEINÄNEN-KIUKAANNIEMI S., JOKE-LAINEN J., AUVINEN J., PUUKKA K., RUOKONEN A., JÄRVELIN M.R., TAPANAINEN J.S., FRANKS S., PILTONEN T.T., MORIN-PAPUNEN L.C. 2017. Overweight and obese but not normal weight women with PCOS are at increased risk of Type 2 diabetes mellitus – a prospective, population-based cohort study. *Hum. Reprod.* **32**: 423-431. <https://doi.org/10.1093/humrep/dew329>
- ONALAN G., SELAM B., BARAN Y., CINCIK M., ONALAN R., GÜNDÜZ U., URAL A.U., PABUCCU R. 2005. Serum and follicular fluid levels of soluble Fas, soluble Fasligand and apoptosis of luteinized granulosa cells in PCOS patients undergoing IVF. *Hum. Reprod.* **20**: 2391-2395. <https://doi.org/10.1093/humrep/dei068>
- OU H.T., CHEN P.C., WU M.H., LIN C.Y. 2016. Metformin improved health related quality of life in ethnic Chinese women with polycystic ovary syndrome. *Health Qual. Life Outcomes*. **14**: 119. <https://doi.org/10.1186/s12955-016-0520-9>
- PADMANABHAN V., VEIGA-LOPEZ A. 2013. Animal models of the polycystic ovary syndrome phenotype. *Steroids* **78**: 734-740. <https://doi.org/10.1016/j.steroids.2013.05.004>
- PEITSIDIS P., AGRAWAL R. 2010. Role of vascular endothelial growth factor in women with PCO and PCOS: a systematic

- review. *Reprod. Biomed. Online* **20**: 444-452. <https://doi.org/10.1016/j.rbmo.2010.01.007>
- POORNIMA R., SARANYA P., BHUVANESHWARI S., AVERAL H. I. 2015. Evaluation of *Pergularia daemia* and metformin in the treatment of PCOS in testosterone propionate induced albino wistar rats (*Rattus norvegicus*). *Int. J. Pharma. Sci. Res.* **6**: 1250-1256.
- QIANG G.F., ZHANG L., XUAN Q., YANG X.Y., SHI L.L., ZHANG H.A., CHEN B.N., DU G.H. 2010. Effect of metformin on the formation of hepatic fibrosis in type 2 diabetic rats. *Acta Pharm. Sin.* **45**: 801-806. (In Chinese with English abstract).
- ROJAS J., CHÁVEZ-CASTILLO M., BERMÚDEZ V. 2014. The Role of metformin in Metabolic Disturbances during Pregnancy: Polycystic Ovary Syndrome and Gestational Diabetes Mellitus. *Int. J. Reprod. Medicine* **2014**: 1-14. <http://dx.doi.org/10.1155/2014/797681>
- ROMÃO L.F., MENDES F.A., FEITOSA N.M., FARIA J.C.O., COELHO-AGUIAR J.M., DE SOUZA J.M., MOURA NETO V., ABREU J.G. 2013. Connective tissue growth factor (CTGF/CCN2) is negatively regulated during neuronglioblastoma interaction. *PLoS One* **8**: e55605. <https://doi.org/10.1371/journal.pone.0055605>
- SABATINI M.E., GUO L., LYNCH M.P., DOYLE J.O., LEE H., RUEDA B.R., STYER A.K. 2011. Metformin therapy in a hyperandrogenic anovulatory mutant murine model with polycystic ovarian syndrome characteristics improves oocyte maturity during superovulation. *J. Ovarian. Res.* **4**: 8. <https://doi.org/10.1186/1757-2215-4-8>
- SALVETTI N., CANAL A.M., GIMENO E.J., ORTEGA H.H. 2004. Polycystic ovarian syndrome: temporal characterization of the induction and reversion process in an experimental model. *Braz. J. Vet. Res. Anim. Sci.* **41**: 389-395. <https://doi.org/10.1590/S1413-95962004000600006>
- SANGRAULA H., PAUDEL K.R., SHARMA M. 2009. Metformin and troglitazone in the treatment of female infertility associated with polycystic ovarian syndrome. *J. Nepal. Med. Assoc.* **48**: 335-339.
- SIVALINGAM V.N., MYERS J., NICHOLAS S., BALEN A.H., CROSBIE E.J. 2014. Metformin in reproductive health, pregnancy and gynaecological cancer: established and emerging indications. *Hum. Reprod. Update.* **20**: 853-868. <https://doi.org/10.1093/humupd/dmu037>
- STAHMANN N., WOODS A., SPENGLER K., HESLEGRAVE A., BAUER R., KRAUSE S., VIOLLET B., CARLING D., HELLER R. 2010. Activation of AMP-activated protein kinase by vascular endothelial growth factor mediates endothelial angiogenesis independently of nitric-oxide synthase. *J. Biol. Chem.* **285**: 10638-10652. <https://doi.org/10.1074/jbc.M110.108688>
- SUN J., JIN C., WU H., ZHAO J., CUI Y., LIU H., WU L., SHI Y., ZHU B. 2013. Effects of electro-acupuncture on ovarian P450arom, P450c17a and mRNA expression induced by letrozole in PCOS rats. *PLoS One* **8**: e79382. <https://doi.org/10.1371/journal.pone.0079382>
- TAKEUCHI K., MORIZANE Y., KAMAMI-LEVY C., SUZUKI J., KAYAMA M., CAI W., MILLER J.W., VAVVAS D.G. 2013. AMP-dependent kinase inhibits oxidative stress-induced caveolin-1 phosphorylation and endocytosis by suppressing the dissociation between c-Abl and Prdx1 proteins in endothelial cells. *J. Biol. Chem.* **288**: 20581-20591. <https://doi.org/10.1074/jbc.M113.460832>
- TANG T., LORD J.M., NORMAN R.J., YASMIN E., BALEN A.H. 2012. Insulin-sensitizing drugs (metformin, rosiglitazone, pioglitazone, D-chiro-inositol) for women with polycystic ovary syndrome, oligoamenorrhoea and subfertility. *Cochrane Database Syst. Rev.* **16**: CD003053. <https://doi.org/10.1002/14651858.CD003053.pub5>
- TOBLI J.E., CAO G., OLIVERI L., ANGEROSA M. 2012. Comparison of oxidative stress and inflammation induced by different intravenous iron sucrose similar preparations in a rat model. *Inflamm. Allergy Drug Targets* **11**: 66-78. <https://doi.org/10.2174/187152812798889358>
- TSO L.O., COSTELLO M.F., ALBUQUERQUE L.E.T., ANDRILO R.B., FREITAS V. 2009. Metformin treatment before and during IVF or ICSI in women with polycystic ovary syndrome. *Cochrane Database Syst. Rev.* **2**: CD006105. <https://doi.org/10.1002/14651858.CD006105.pub2>
- VELTMAN-VERHULST S.M., BOIVIN J., EIJKEMANS M.J.C., FAUSER B.J.C.M. 2012. Emotional distress is a common risk in women with polycystic ovary syndrome: a systematic review and meta-analysis of 28 studies. *Hum. Reprod. Update* **18**: 638-651. <https://doi.org/10.1093/humupd/dms029>
- VRBIKOVA J., HAINER V. 2009. Obesity and polycystic ovary syndrome. *Obes. Facts* **2**: 26-35. <https://doi.org/10.1159/000194971>
- WALLACE T.M., LEVY J.C., MATTHEWS D.R. 2004. Use and abuse of HOMA modeling. *Diabetes Care.* **27**: 1487-1495. <https://doi.org/10.2337/diacare.27.6.1487>
- WALTERS K.A., ALLAN C.M., HANDELSMAN D.J. 2012. Rodent models for human polycystic ovary syndrome. *Biol. Reprod.* **86**: 149, 1-12. <https://doi.org/10.1095/biolreprod.111.097808>
- WANDJI S.A., GADSBY J.E., BARBER J.A., HAMMOND J.M. 2000. Messenger ribonucleic acids for MAC25 and connective tissue growth factor (CTGF) are inversely regulated during folliculogenesis and early luteogenesis. *Endocrinology* **141**: 2648-2657. <https://doi.org/10.1210/endo.141.7.7576>
- WANG D., WANG W., LIANG Q., HE X., XIA Y., SHEN S., WANG H., GAO Q., WANG Y. 2018. DHEA-induced ovarian hyperfibrosis is mediated by TGF- β signaling pathway. *J. Ovarian Res.* **11**: 6. <https://doi.org/10.1186/s13048-017-0375-7>
- WU Y., LI P., ZHANG D., SUN Y. 2018. Metformin and pioglitazone combination therapy ameliorate polycystic ovary syndrome through AMPK/PI3K/JNK pathway. *Exp. Ther. Med.* **15**: 2120-2127. <https://doi.org/10.3892/etm.2017.5650>
- YI Q.Y., DENG G., CHEN N., BAI Z.S., YUAN J.S., WU G.H., WANG Y.W., WU S.J. 2016. Metformin inhibits development of diabetic retinopathy through inducing alternative splicing of VEGF-A. *Am. J. Transl. Res.* **8**: 3947-3954.
- ZHANG X., ZHANG C., SHEN S., XIA Y.J., YI L., GAO Q., WANG Y. 2013. Dehydroepiandrosterone induces ovarian and uterine hyperfibrosis in female rats. *Hum. Reprod.* **28**: 3074-3085. <https://doi.org/10.1093/humrep/det341>
- ZHAO M., CHANG C., LIU Z., CHEN L.M., CHEN Q. 2010. The level of vascular endothelial cell growth factor, nitric oxide, and endothelin-1 was correlated with ovarian volume or antral follicle counts: A potential predictor of pregnancy outcome in IVF. *Growth Factors* **28**: 299-305. <https://doi.org/10.3109/08977191003766866>
- ZHOU F., SHI L.B., ZHANG S.Y. 2017. Ovarian Fibrosis: A Phenomenon of Concern. *Chin. Med. J.* **130**: 365-371. <https://doi.org/10.4103/0366-6999.198931>
- ZHOU H., OHNO N., TERADA N., SAITOH S., NAITO I., OHNO S. 2008. Perms electivity of blood follicle barriers in mouse ovaries of the mifepristone-induced polycystic ovary model revealed by in vivo cryotechnique. *Reproduction* **136**: 599-610. <https://doi.org/10.1530/REP-08-0022>